AFC73174

prepared for the
National Institutes of Health
National Institute of Neurological Disorders and Stroke
Neural Prosthesis Program
Bethesda, Maryland 20892

# ELECTRODES FOR FUNCTIONAL ELECTRICAL STIMULATION

**Contract #NO1-NS-6-2346**

**Technical Progress Report #2**
**January 1, 1997 - April 30, 1997**

Principal Investigator
J. Thomas Mortimer, Ph.D.

Applied Neural Control Laboratory
Department of Biomedical Engineering
Case Western Reserve University
Cleveland, OH USA

# TABLE OF CONTENTS

..... page

SECTION B. DESIGN AND FABRICATION OF ELECTRODES, LEADS AND CONNECTORS

B.2.1.2: Polymer-Metal Foil-Polymer (PMP) Cuff Electrodes....3
B.2.2: Lead Designs ...11

SECTION C. IN VIVO EVALUATION OF ELECTRODES

C.1: Electrode Selectivity ...20

## SECTION B. DESIGN AND FABRICATION OF ELECTRODES, LEADS AND CONNECTORS

### B.2.1.2: Polymer-Metal Foil-Polymer (PMP) Cuff Electrodes

The polymer-metal foil-polymer (PMP) electrode is a novel design that attempts to improve the mechanical reliability and ease the manufacturing process of spiral nerve cuff electrodes. The electrode design relies upon laser micromachining technology applied to both metal foils and polymer-metal foil laminates. In order to better understand lasers and their application to machining, personnel from our lab attended a day long technology seminar hosted by a leading contract laser micromachining supplier.

Over the course of this contract, we have worked with PI Medical of Portland, OR in developing and implementing strategies for the fabrication of this electrode. Preliminary technical issues that have been raised and resolved were reported in a previous technical progress report (TPR #1). In recent months, a CAD drawing for the PMP design was generated and initial efforts have been made at fabricating prototype PMP electrodes in both the 25 and 50μm thick platinum foils. Additionally, alternative sources for the laser machining have been approached and efforts are underway with these alternative sources.

Laser Seminar

The PMP electrode requires micromachining of both metal foils and metal foil-polymer structures. Micromachining techniques that were preliminarily investigated included lasers, electrical discharge machining and chemical etchants. The latter 2 techniques as well as more traditional types of machining were not feasible for use with the PMP electrode. Laser machining presents several advantages for our application. Lasers are non-contacting, which eliminates tool wear concerns but more importantly makes them applicable to materials such as ceramics and polymers that are traditionally more difficult to machine. Laser machining involves no solvent chemicals, so disposal and chemical handling are not a concern. Lasers allow for selective material removal through adjustments in laser power and intensity. This is particularly advantageous for use with the PMP electrode, where selective removal of the silicone rubber overlying the platinum foil is to be performed. Finally, because laser machining systems are computer controlled, the technique is very flexible and changes to design or dimensions are easily accommodated.

An engineer from our lab attended a day-long laser micromachining seminar in March 1997. This seminar was hosted by Resonetics, Inc. (Nashua, NH) and was led by their director of corporate development, Ron Schaeffer, Ph.D. The seminar was intended as a technology seminar, not a sales seminar, aimed at persons with an interest in but little knowledge of laser micromachining. The topics covered in the seminar included: introduction to laser technology, overview of each laser type, beam delivery techniques, system components and integration, and applications. The seminar provided an opportunity to learn more about specific laser types and the advantages and disadvantages of each. This knowledge will help to select the appropriate laser type for use with the PMP electrode and anticipate the technical limitations of our laser processor(s).

Three types of lasers are commonly used for laser micromachining applications. These are the solid state Nd-YAG (neodinium doped yttrium aluminum garnet) laser, the CO2 gas laser and excimer gas lasers. These lasers are classified based on the medium used within the laser cavity to generate the laser beam, which may be solids, gases or liquids. Excimer (shortened from excited dimer) lasers are gas lasers that use combinations of rare or noble gases as the lasing medium, including ArF, KrF, and XeCl. Nd-YAG and CO2 lasers are well-developed technologies and are widely available for purchase or contract services. Excimer lasers are an emerging technology and are becoming more and more frequent in micromachining applications. A comparison of these lasers is provided in the following table.

## Table B.1.1: Comparison of Laser Types

| Laser Type | Development Status | Wave-length | Resolution Limit | Side Effects | Material Interaction |
|---|---|---|---|---|---|
| Nd:YAG | high | 1.064 μm (IR) | 25 μm | recast layer, burring, thermal | thermal |
| $CO_2$ | high | 9.4-11.0 μm (IR) | 50 μm | recast layer, burring, thermal | thermal |
| Excimer (noble gas) | low | 0.193-0.351 μm (UV) | 5 μm | recast layer | photoablation, thermal |

In the PMP electrode, we are concerned primarily about the precision of the machined cuts. Additionally, the compatibility of the laser with our materials and the residual effects of the laser on our electrode materials is a significant issue. At this time, power and the ability for mass production is of minor importance.

The resolution limit of features machined by each laser is theoretically defined by the wavelength of the laser. However, in practical terms, the resolution limit is several times the wavelength. Nd-YAG lasers have a wavelength of 1.064μm and a practical resolution limit of 20-30μm; CO2 lasers have a wavelength of 10.6μm and a practical resolution limit of 50μm; excimer lasers have wavelengths in the range 0.193-0.351μm and practical resolution limits of 5μm. Based on this, we would not expect CO2 lasers to be capable of machining our PMP design, which has features on the order of 50μm. The Nd-YAG laser may be capable of producing the features required in the PMP design, but may be stretched to its resolution limits. By using a technique known as frequency doubling, in which the laser beam is passed through a prism, the wavelength of the Nd-YAG laser can be halved and resolution improved. The frequency doubling can be repeated multiple times, further decreasing the wavelength of the laser. However, with each frequency doubling, the power of the laser beam is also halved. The resolution required for the PMP electrode is well within the capabilities of excimer lasers.

In laser machining, the material of the workpiece is removed through either thermal or ablative processes. The method of material removal is dependent on both the characteristics of the laser and of the workpiece material. When the photons of the laser beam interact with the workpiece, energy is transferred and the workpiece molecules and atoms become excited. Nd-YAG and CO2 lasers operate in the infra-red (IR) region of the electromagnetic spectrum, while the excimer lasers operate in the ultra-violet (UV) region. Photons in the IR region are at lower energy than photons in the UV region. At wavelengths in the IR region, the energy of the photons generally increases the kinetic energy of the atoms or molecules in the workpiece and results in heating through increased vibrations of the molecules. Material removal on the workpiece is a result of thermal processes. At wavelengths in the UV region, the energy of the photons is higher, and in some cases is greater than the bond energies between the molecules in the workpiece. In these cases, when the photons of the laser interact with the workpiece, the molecular bonds are broken directly and what is known as 'ablation' occurs. However, the method of material removal is also dependent on the characteristics of the workpiece. For metals, the molecular bond energies are higher than those emitted by lasers in the UV region, and so the photons of the laser generate heating, and subsequent material removal through thermal processes. For polymers and other materials with lower bond energies, lasers in the UV region are ablative.

In the PMP electrode, both metal foils and polymers are to be machined. Thermal material removal methods can be expected to result in decreased edge definition as compared to ablative material removal. Additionally, thermal processes can potentially alter material structure and properties in surrounding regions of the machined feature, similar to the heat affected zones seen

surrounding welds. Ablation of our workpiece, would then seem the ideal method. However, because we are working with metals, removal of the foil will be through a thermal process. Ablation of the polymer portion of the PMP electrode is possible and will depend on laser selection. To reduce residual thermal effects on the workpiece and to improve edge definition around machined features, laser systems are often outfitted with gas jets in the vicinity of the workpiece. The gas acts to cool the workpiece, carry away molten material, and prevent oxidation or other chemical reactions from occurring at the workpiece surface.

Ablation of the polymer portions of the PMP electrode would seem desirable and would suggest the use of an excimer laser for this portion of the machining. However, as mentioned above, excimer lasers operate in the UV spectrum. The PMP electrode is a laminated structure of platinum foil and silicone rubber. It has been suggested that UV exposure is damaging to the long-term reliability of silicone rubber. If a UV laser is selected for machining of the silicone rubber, special attention will be paid to the silicone rubber in the areas surrounding the machined features. Specific long-term reliability testing of laser-machined silicone rubber may be implemented.

While the laser beam is the actual machining tool, precision micromachining requires well-developed laser systems. In addition to the laser itself, these systems can include beam delivery schemes that use various optics, beam splitters, etc to bring the laser beam to the workpiece, auxiliary devices such as cameras, microscopes and gas jets and workpiece positioning mechanisms that both place the workpiece initially and then provide for movement of the workpiece or laser during machining. Computer control is integral for precision micromachining. Systems such as these can be purchased for $100-300K, or are available through contract machining services.

PI Medical is one such contract machining provider. PI Medical uses a Nd-YAG laser and expects to be able to machine the PMP electrode to our specifications. This suggests that they use a frequency doubling method to improve the resolution achievable with their solid-state laser beam.

CAD Drawing/CAM File

Laser machining, particularly to tight dimensional requirements like those of the PMP electrode, necessitates computer control. This in turn requires that the design be inputed to computer drawing software, such as AutoCAD. We have previously generated schematics of the electrode design and specified dimensions of features within the design. However, our schematic drawings were not compatible with AutoCAD, which requires very precise dimensioning and positioning. Our colleagues at PI Medical are familiar with AutoCAD and the generation of design specifications within the program. After providing them with specific dimensions, we contracted with PI Medical to produce an AutoCAD file of the PMP design.

We have selected dimensions for the PMP electrode based on our expectations of the material behavior and based on previous experience with foils. However, these dimensions are subject to change based on the laser capabilities and resulting flexibility of the electrode substrate. Additionally, dimensions and spacing of the electrode contacts will be dependent on desired cuff size. For our prototyping work, the PMP design is based on a 3 mm diameter nerve cuff, 3 mm being the average diameter of the cat sciatic nerve. Spacing of the contact pads, intended to be 90° offset from one another, and numbers of slots machined between each contact pad is determined by cuff diameter.

PI Medical was provided the desired dimensions of our PMP prototype. An important point we had not considered in the generation of the CAD drawing is an accounting for the diameter of the laser beam. Dimensions of desired features must consider that while the laser beam will be focused on the line of the drawing, half of the width of the beam will be spread to either side. The dimensions and spacing of the features must account for this non-finite sized machine tool.

The CAD drawing was quickly completed by PI Medical and a disk copy of the file sent to us. Minor revisions to the file were made to comply with our design specifications. The CAD file contains 4 'layers', which are the individual steps in the laser machining production of the PMP electrode. In the first layer, the pattern of holes to be machined through the platinum foil is made. Additionally in this step, the re-alignment markers are machined in the foil outside the electrode

area. The second layer involves the cuts that isolate each electrode pathway and that are machined through the foil-polymer laminate structure. The final two steps are the ablation of the polymer in the areas of the bonding and contact pads and the cutting of the outer dimensions of the electrode.

Prototype

PI Medical has performed the initial step in fabricating the PMP electrode: the first pass of laser cuts that create the pattern of holes throughout the platinum foil piece. Prototypes in both 25 and 50µm foils have been made. These prototypes were returned to us for evaluation and performance of the next fabrication step, the lamination of the foil in silicone rubber.

Each prototype was examined with a light microscope and a scanning electrode microscope (SEM). At the light level, slight discoloration of the 50µm foil immediately surrounding the slots was observed. No color changes were noted in the 25µm foil. The machining of both pieces appeared to have clean edges and less burring than that seen in the preliminary machining samples (see TPR#1). SEM evaluation provided confirmation of the good edge definition for both sample thicknesses. Additionally, no color changes were noted in either sample using the SEM. Photomicrographs of these prototypes are presented in Figures B.2.1.1-6.

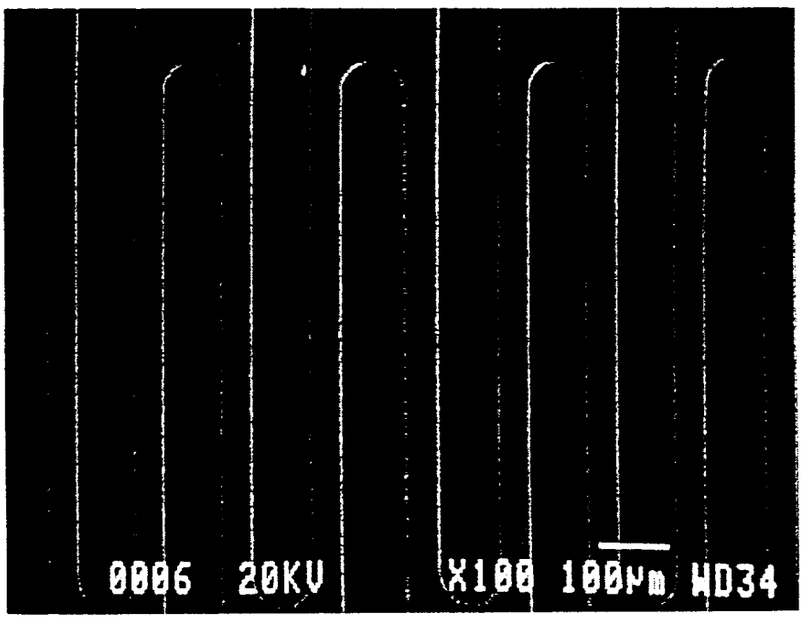


**Figure B.2.1.1:** SEM photomicrograph of 25µm foil PMP prototype. The patterned slots are evenly spaced and have good edge definition.

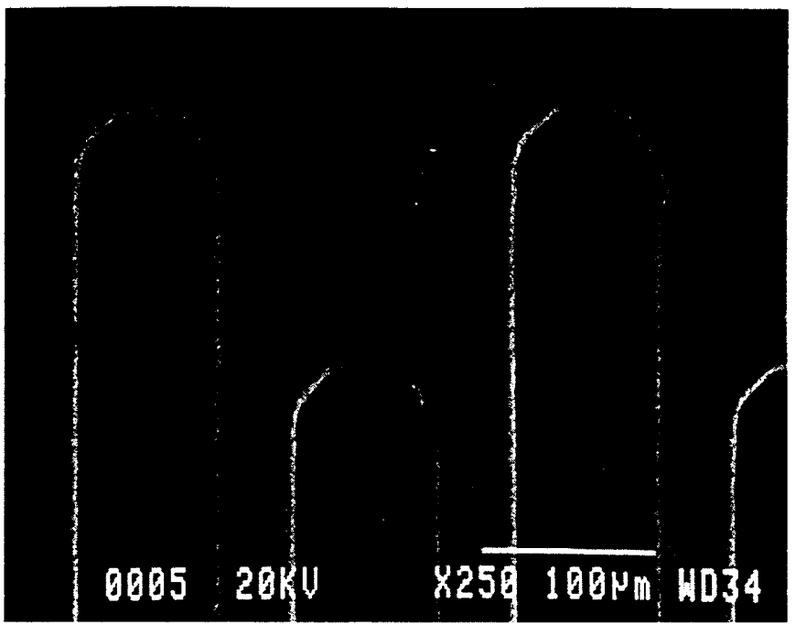


**Figure B.2.1.2:** SEM photomicrograph of 25µm foil PMP prototype. Details of the machined slots are shown, with only a slight ridge of metal surrounding each slot.

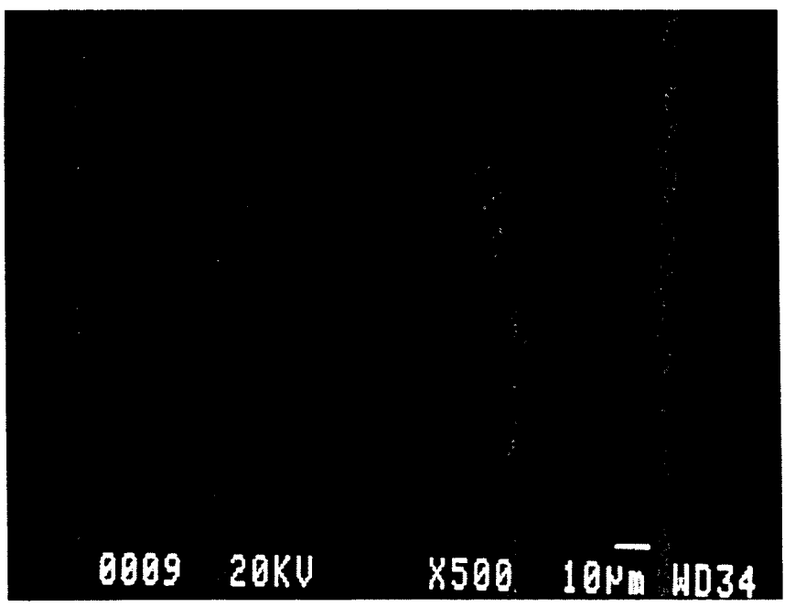


**Figure B.2.1.3:** SEM photomicrograph of 25µm foil PMP prototype. At this high magnification view, the ridge of foil at the periphery of each slot appears to be low and rounded. Possible re-deposited material is noted in regions outside of the slots.

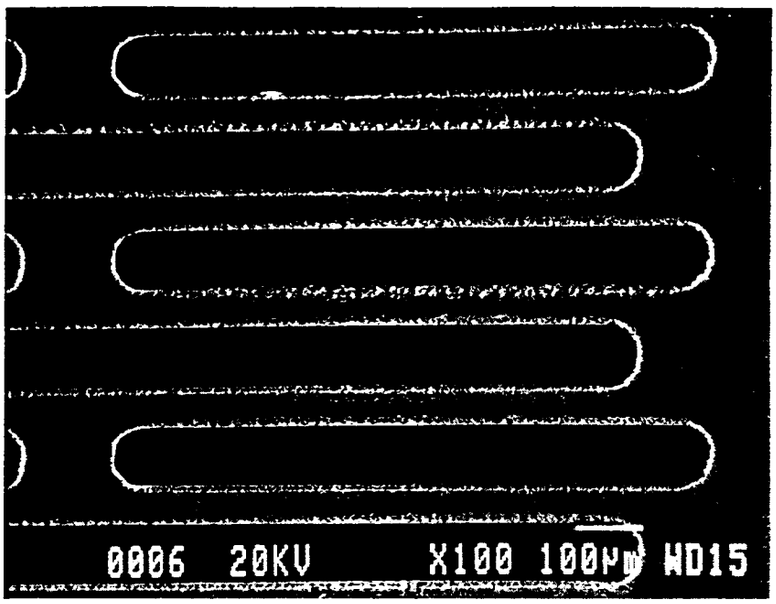


**Figure B.2.1.4:** SEM photomicrograph of 50µm foil PMP prototype. Again, the patterned slots are evenly spaced and have good edge definition.

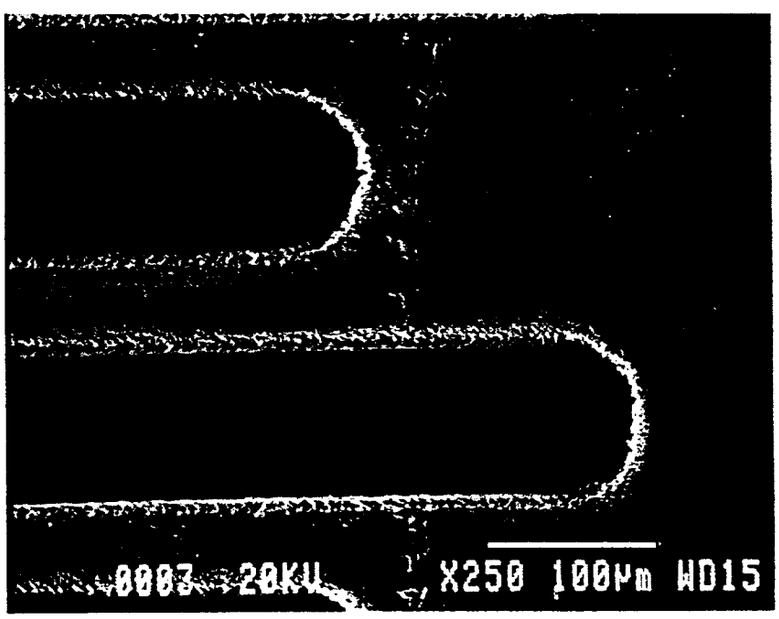


**Figure B.2.1.5:** SEM photomicrograph of 50µm foil PMP prototype. Details of the machined slots are shown, with only a slight ridge of metal surrounding each slot.

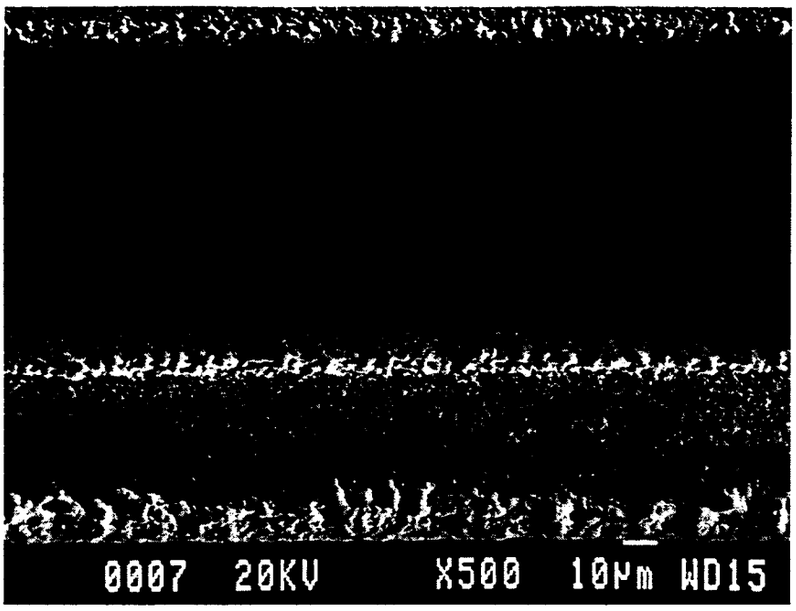


**Figure B.2.1.6:** SEM photomicrograph of 50µm foil PMP prototype. At this high magnification view, the ridge of foil at the periphery of each slot appears to be low and rounded. Possible re-deposited material is noted in regions outside of the slots.

Now that the first pass of laser cuts has been made, the next step is to laminate the foil in silicone rubber. Our intention is to follow the general procedure we use to make a spiral cuff: sandwiching uncured silicone elastomer and the platinum foil between 2 layers of pre-formed silicone rubber sheeting. For the lamination, the top layer of silicone rubber sheeting will not be stretched, as we do not want the laminated piece to form a self-wrapping spiral. While this is our initial plan for lamination, we do have some concerns regarding its potential for success.

First, we are unsure of how well the uncured elastomer will spread to fill all of the voids in the platinum foil. Air bubbles and incomplete filling of the voids will not provide the stable structure that is required for the second pass of laser cuts. We will pay particular attention to how we spread the elastomer, minimizing and forcibly removing visible air bubbles. We will also attempt to incrementally apply pressure to the plates, allowing the elastomer to gently and slowly spread to the final thickness of the laminated structure. Rapid application of pressure may result in squirting of the elastomer to the perimeter of the plates. Rapid movement of the elastomer would increase the likelihood of bubbles being trapped in the interior of the laminated structure and may result in enough shear forces to cause deformation of the platinum foil, particularly the spans of foil left between subsequent machined slots.

Our second concern regarding the lamination procedure is our ability to produce an even thickness coating over the platinum foil. The success of the subsequent laser machining, particularly the ablation step to expose the contact and bonding pads, will be highly dependent on the consistency in thickness of the silicone rubber. Shim stock, placed between the plates that will be used for the lamination, serves to define the thickness of the final laminated structure. This shim stock can be chosen to a minimum of twice the thickness of the sheeting plus the thickness of the foil. However, this provides for no tolerance and minimizes the amount of elastomer that is left surrounding the platinum foil and essentially holding the laminated structure together. If we choose a shim thickness that is significantly greater than our minimum, we risk producing an inconsistent thickness of elastomer between the top layer of sheeting and the foil (and subsequently between the bottom layer of sheeting and the foil). If viewed from the side, the foil may appear to ripple or ramp between the top and bottom sides of the sheeting. This will interfere with the precision and success of future laser machining. We will first attempt to use the minimal thickness shim stock possible to avoid inconsistency in planar location of the foil within the laminate. If this zero tolerance approach is not successful and the lamination procedure fails, we will then use a shim stock thickness that is slightly greater than the minimal required, projected to be an additional 25μm.

Initial attempts at lamination will be performed on sample machined pieces of foil. This will allow us to test our hypotheses of the optimal lamination technique without ruining our prototypes. Once we have laminated both prototype foils, we will return them to PI Medical for the second pass of laser cuts. These cuts are precision, discrete cuts that will serve to isolate each electrode pathway. If these cuts are misaligned or out of position relative to the patterned foil, isolation may not be achieved and/or the structure may not remain intact. Upon completion of the second pass of laser cuts, the foil will again be returned to us for evaluation. The flexibility of the laminated structure will be evaluated qualitatively. Additionally, the prototypes will be examined microscopically for the placement, precision, and cleanliness of the second laser cuts.

## B.2.2: Lead Designs

The fluoropolymer insulated wire that we have used for intramuscular electrodes has proven to be safe and reliable. However, the appropriateness of this wire for use with cuff electrodes and connectors that are made from silicone rubber is in question. The fluoropolymer does not adhere well to silicone rubber. Poor bonding between these two materials may lead to early mechanical failure of the components, as well as early corrosion through electrolyte seepage at the material interfaces. We have begun investigating the feasibility of applying a coating of silicone rubber over the fluoropolymer insulated wire. The silicone rubber overcoating will provide an additional layer of insulation and protection to the stainless steel wires and will also provide a compatible material surface for bonding with silicone rubber cuffs and connectors.

### PI Medical Wire

In the early months of this contract, we began working with PI Medical of Portland, OR to perform the silicone rubber overcoating of our wire. Details of our initial work were provided in a previous report (see TPR #1). PI Medical's first effort at overcoating our wire resulted in a silicone rubber coating that flaked off the fluoropolymer jacket when stressed due to its low mechanical strength . Using a NuSil silicone rubber formulation, PI Medical was able to provide us with a second attempt at the silicone rubber overcoating. An approximately 2 mil thickness of NuSil MED-4950 silicone rubber elastomer was extruded over our standard wire. Samples of the wire were wound on a mandrel, as would be done during lead manufacture. While the material was not observed to flake off, it was noted that the wound cable adhered to the hard steel mandrel and was difficult to remove from the mandrel. Uncoiled and coiled lengths of the overcoated wire were prepared for SEM evaluation. The coiled wire segments included some that had been forcibly removed from the mandrel and some that had been left on the mandrel.

Photomicrographs of uncoiled wire samples are presented in Figures B.2.2.1-2. Surface contaminants can be seen in several areas and are attributed to inadequate cleaning and handling before SEM evaluation. In addition to the surface contaminants, some surface defects in the silicone rubber overcoat can be noted, particularly in Figure B.2.2.1. At high magnifications these defects appear to be shallow furrows in the jacketing and were found frequently in the sample segments examined.

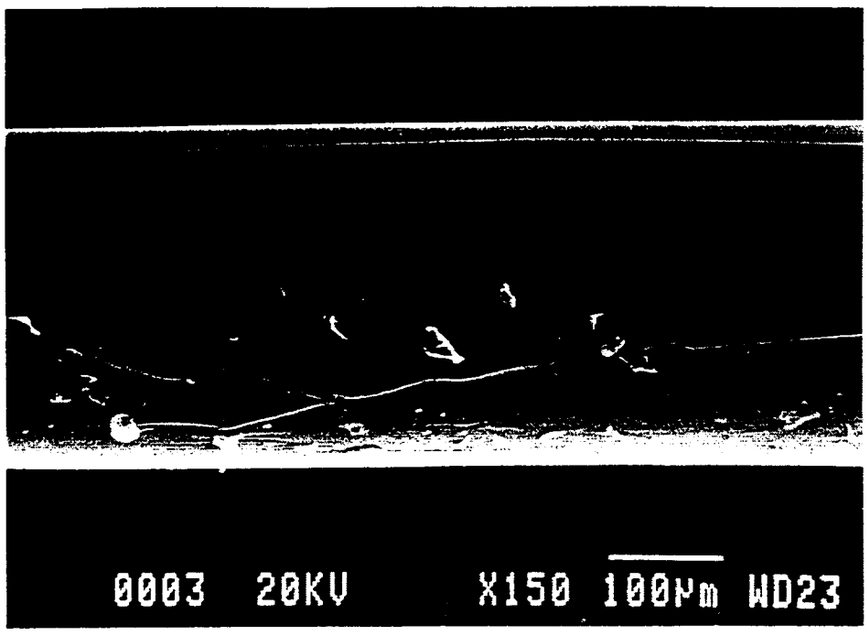


**Figure B.2.2.1:** SEM photomicrograph of uncoiled silicone rubber coated wire manufactured by PI Medical. A longitudinal furrow in the surface of the silicone rubber overcoat is seen, as are surface contaminants.

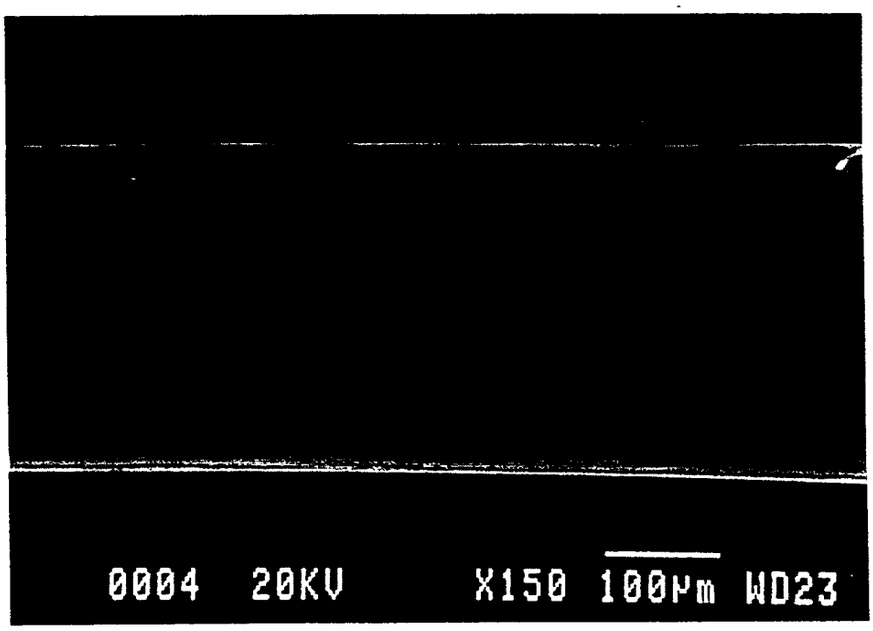


**Figure B.2.2.2:** SEM photomicrograph of uncoiled silicone rubber coated wire manufactured by PI Medical. The wire surface appears largely smooth and free of surface defects.

Multiple wire segments of coils left on the steel mandrel were examined to evaluate the shape and deformation of the overcoated wire in its as-wound state. An example of these coils is presented in Figure B.2.2.3. In this photomicrograph, the overcoated wire appears very similar to our fluoropolymer jacketed wire. The coils are evenly spaced and rounded, with no obvious structural defects in the stressed wire. Small surface features, with an appearance similar to wrinkles or undulations, can be seen on the coiled wire, and appear to be preferentially oriented perpendicular to the wire coil. These features are shown at higher magnification in Figure B.2.2.4. The significance of these markings is unclear, although they may be signals that higher stresses are being applied to the silicone rubber jacketing.

In other coiled wire segments, the mandrel was removed, both forcibly and with the aid of surfactants. The range of coil features seen in these samples is shown in Figures B.2.2.5-6. Some areas of the coil appear to be intact and normal, as seen in Figure B.2.2.5. In other areas, the outer jacketing appears significantly deformed and to be almost pulling entirely off of the underlying fluoropolymer insulation, as in Figure B.2.2.6. Varying degrees of this deformation were seen in other wire sections. It is our belief that the silicone rubber surface adheres to the winding mandrel and that when the mandrel is pulled out, the silicone rubber is pulled along. In some cases, the jacket appears to have actually ruptured; in others it appears to simply be stretched. The silicone rubber surfaces can also adhere to one another and it may be that this adhesion acts to prevent the stretched jacket from returning to a position centered around the fluoropolymer.

Evaluation of this wire has been limited primarily to the microscopic observations described above. The surface "wrinkles' and contaminants are of some concern but are minor issues relative to our concerns about the apparent instability of the outer jacketing when subjected to shear stresses. Plans for additional testing were delayed until a comparison between this wire and that fabricated by Specialty Silicone Fabricators could be made.

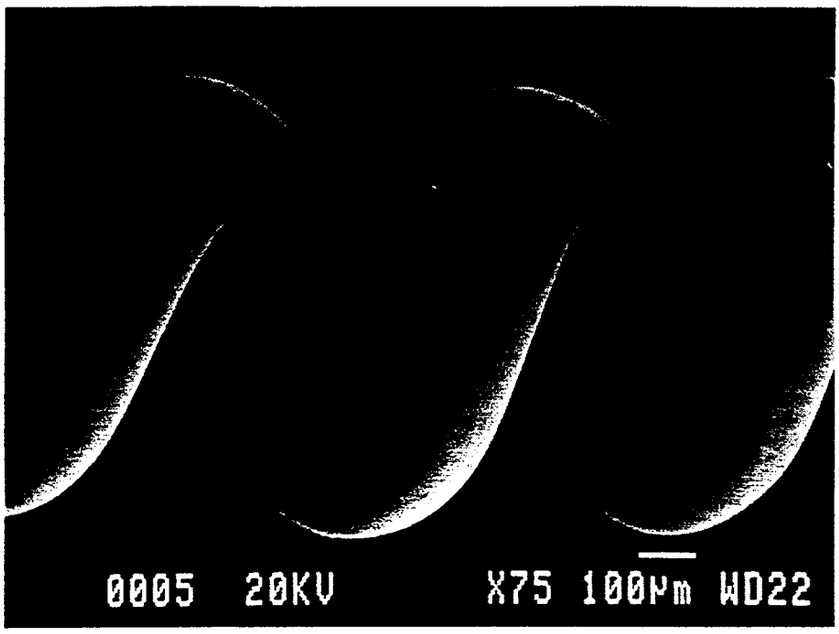


**Figure B.2.2.3:** SEM photomicrograph of PI Medical silicone rubber coated wire wound around a 7 mil mandrel. The coil is well-shaped and even.

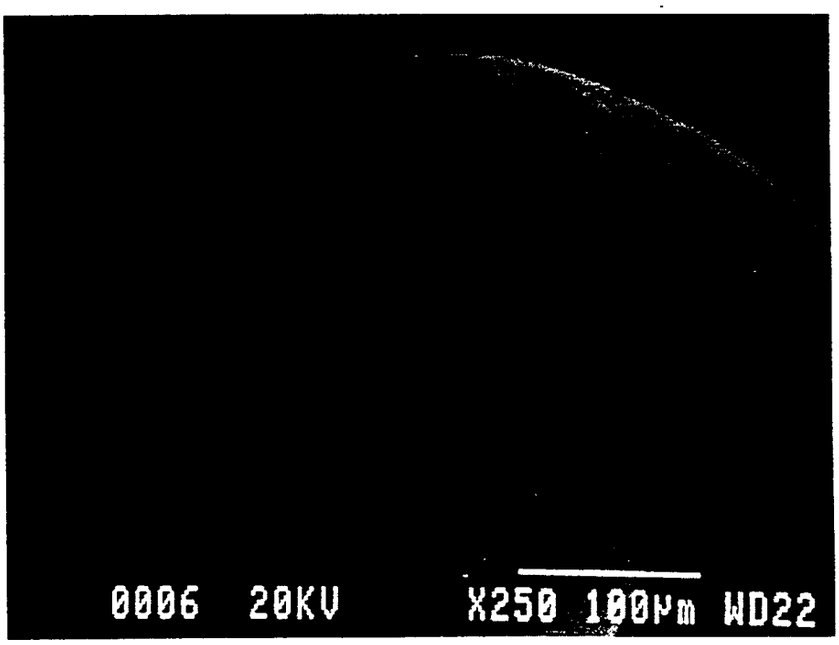


**Figure B.2.2.4:** SEM photomicrograph at high magnification of coil in Figure B.2.2.3. Small surface markings can be seen on the wire and are primarily oriented perpendicularly to the direction of the coil.

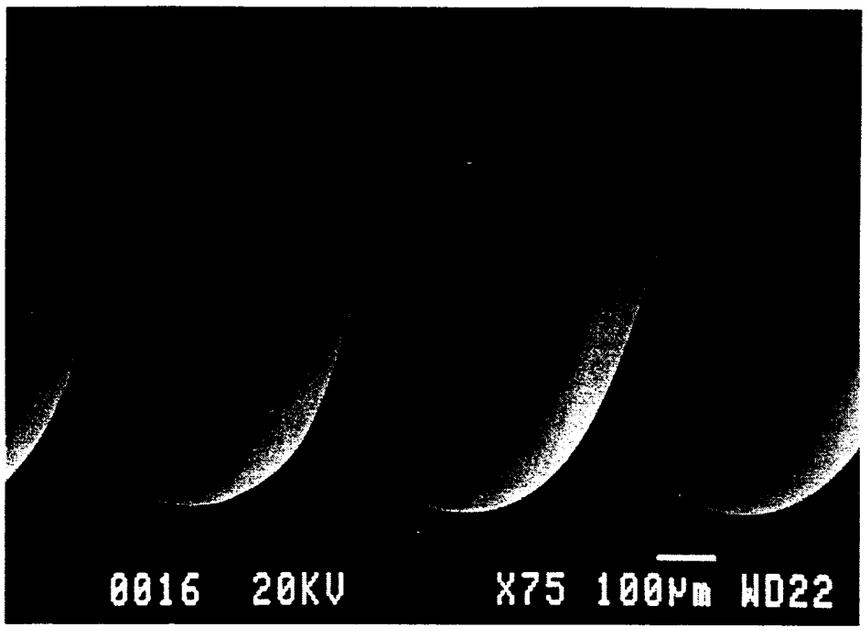


**Figure B.2.2.5:** SEM photomicrograph of PI Medical silicone rubber coated wire wound on a mandrel that has been removed. The coils are similar in appearance to those of Figure B.2.2.3 and are evenly spaced and well-rounded.

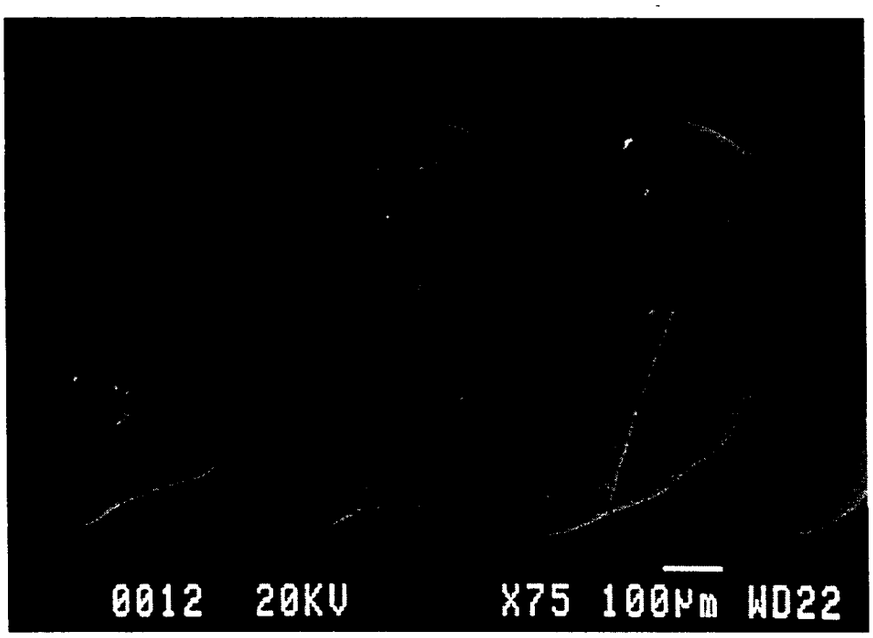


**Figure B.2.2.6:** SEM photomicrograph of PI Medical silicone rubber coated wire wound on a mandrel that has been removed. The silicone rubber appears to have been deformed and fills the spaces between windings.

**Specialty Silicone Fabricators and Corona Etch**

In exploring alternative sources and approaches to this project, we contacted Specialty Silicone Fabricators, the company that manufactures our silicone rubber sheeting. We were advised that to improve the adherence of the silicone rubber overcoating, the fluoropolymer should undergo an etch treatment. The etch process, in this case a corona etch, results in a roughened polymer surface which will not allow for actual chemical bonding between the fluoropolymer and silicone rubber but will improve the mechanical cohesion between the two materials.

Temp-Flex Cable provides a corona etch service of fluoropolymers that is often used to improve material adhesion, particularly for markings and ink application. Fluoropolymers in thicknesses of 50µm or greater were not expected to be outside the range of Temp-Flex Cable's capabilities. Thicknesses less than this might present problems, as the etch process may penetrate through the entire thickness of the fluoropolymer, compromising insulative and mechanical integrity. A 200' length of our lead wire with a nominal fluoropolymer insulation of 50µm was sent to Temp-Flex Cable with the intent that half the length would be exposed to the corona etch process.

After etching, the wire sample was directed to Specialty Silicone Fabricators for coextrusion of silicone rubber. The material chosen for the coextrusion was NuSil's MED-4750, as recommended by Specialty Silicone Fabricators personnel. The coextrusion was predicted to result in a minimal thickness of 50-75µm silicone rubber jacket. This material has recently been received, minus a significant length (110') that was lost in initial set-up and parameter adjustment. Microscopic observation of uncoiled and coiled wire segments has begun.

Small surface defects and surface contaminants were noted in uncoiled wire lengths, as depicted in Figures B.2.2.7-8.

Lengths of wire were coiled around a 9 mil mandrel and then placed in surfactant to aid in removal of the mandrel. Examples of these wire samples are shown in Figures B.2.2.9-10. The coiled wire segments depicted in the figures were wound with a relatively high pitch and resulted in the very open helix seen in the photomicrographs. Small surface defects, including pinholes and longitudinal surface cracks, can be noted on the coiled wires. Additionally, some folding of the silicone rubber at the inside of the coils is apparent. It is not clear whether these are a direct result of the coiling process, or are related to the removal of the mandrel.

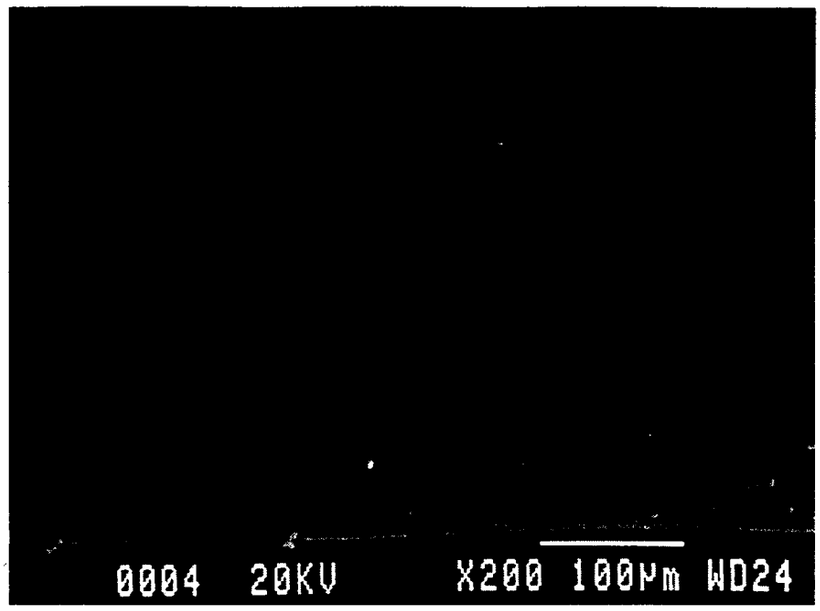


**Figure B.2.2.7:** SEM photomicrograph of uncoiled silicone rubber coated wire manufactured by Specialty Silicone Fabricators. Surface contaminants, as well as surface defects such as pinholes can be seen in the silicone rubber coating.

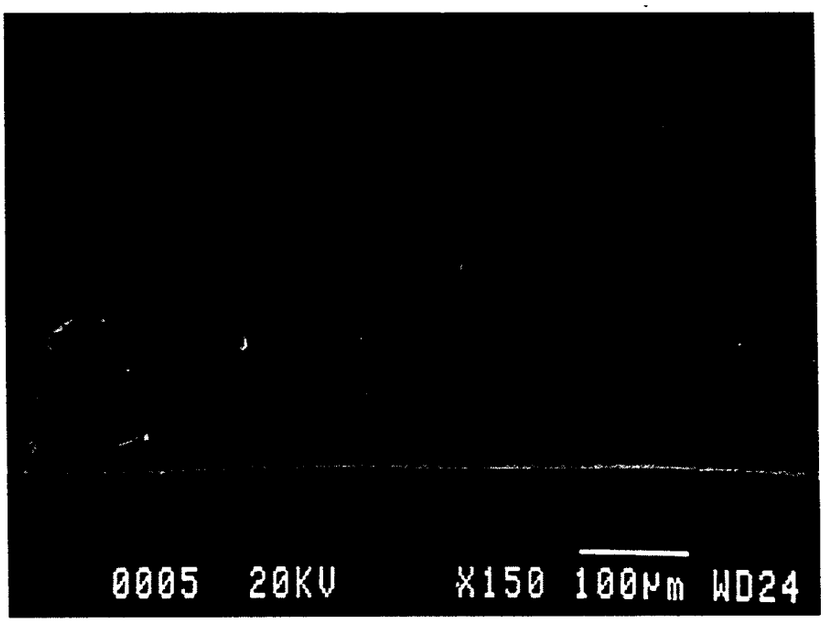


**Figure B.2.2.8:** SEM photomicrograph of uncoiled silicone rubber coated wire manufactured by Specialty Silicone Fabricators. Small surface defects can be seen in the silicone rubber overcoat.

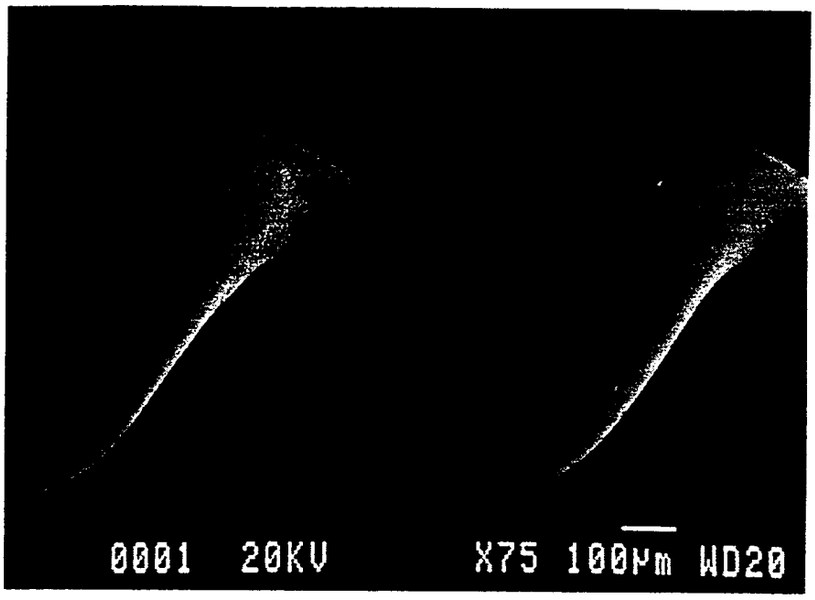


**Figure B.2.2.9:** SEM photomicrograph of Specialty Silicone Fabricator silicone rubber coated wire wound on a 9 mil mandrel that has been removed. The wire was wound at a high pitch angle which resulted in the increased spacing between subsequent windings.

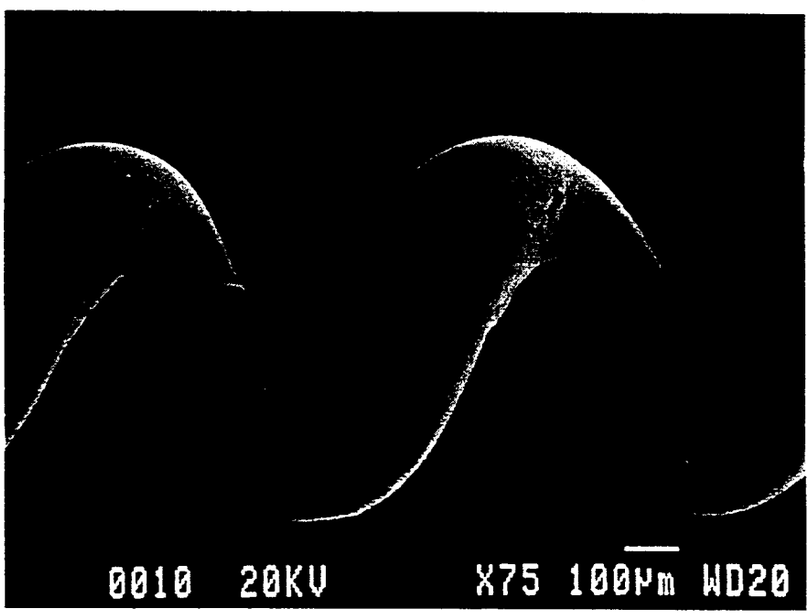


**Figure B.2.2.10:** SEM photomicrograph of Specialty Silicone Fabricator silicone rubber coated wire wound on a 9 mil mandrel that has been removed. The silicone rubber on the insides of the windings appears to be folded.

Future Work

In the coming months, we will continue to evaluate these wire samples and begin to compare their performance. Additional coils of the Specialty Silicone Fabricators wire will be manufactured to create a tighter helix that can be more accurately compared to the coils of PI Medical wire. Additional testing that will be performed in future months include mechanical, electrical and in vitro aging tests. Anecdotal observations of the handling and behavior of the wire will also contribute to our future plans for incorporation of this wire in implant components.

# SECTION C. IN VIVO EVALUATION OF ELECTRODES

## C.1: Electrode Selectivity

Abstract

The purpose of this project is to demonstrate that "field steering" can be used to isolate electrical excitation to individual fascicles in a nerve trunk. During this reporting period we have conducted three acute animal experiments focused on isolating the activation of the lateral gastrocnemius/soleus fascicle from the medial gastrocnemius fascicle when one of the four contacts in the monopolar electrode was positioned to activate both branches together. The results of the studies showed that "field steering" was effective in isolating the two branches. The mechanism for this isolation, however, was not immediately apparent. We speculated that either experimental error (polarity reversal) or an incomplete understanding of the mechanism of "field steering" are responsible. We have not been able to identify experimental error as the problem and have focused on understanding the excitation current pattern in an effort to explain our results and build a procedure to separate excitation of specific fascicles. We also provide a potential configuration for how an implantable stimulator can be configured to effect "field steering".

### Purpose

The purpose of this project is to demonstrate that "field steering" can be used to isolate excitation to individual fascicles in a nerve trunk.

### Progress

During this reporting period we have conducted three acute animal experiments that focused on isolating the activation of the lateral gastrocnemius/soleus fascicle from the medial gastrocnemius fascicle when one of the four contacts in the monopolar electrode was positioned to activate both branches together. The results of the first experiment are shown in figure C.1, where the resulting torque vectors for each of the four main branches (common peroneal, tibial, medial gastrocnemius and lateral gastrocnemius / soleus) are shown in a light gray and labeled. The cuff electrode in cat#244 was positioned such that one contact, the 270° position, recruited both the medial and lateral gastrocnemius, shown in figure C.1 as the curve for the 270° position (shown with diamonds). The position of that contact was found to lie on the nerve trunk, equally close to both the medial and lateral gastrocnemius fascicles, as shown in the drawing in the lower right portion of figure C.1. The 270° position was then stimulated in conjunction with steering currents from each of the other positions. This steering current consisted of passing positive current from the steering contact (0°, 90° or 180° position in this case) to the stimulating contact (270° position in this case). These three curves are shown in circles, squares and triangles for the 0°, 90°, and 180° positions respectively. The resulting vectors due to the steering current did not produce the expected output directions. Stimulation of the 270° position with steering from the 180° produced a vector output found consistent with the lateral gastrocnemius rather than the medial gastrocnemius, as expected. Stimulation of the 270° position with steering from the 90° position corresponded to vector output found for the

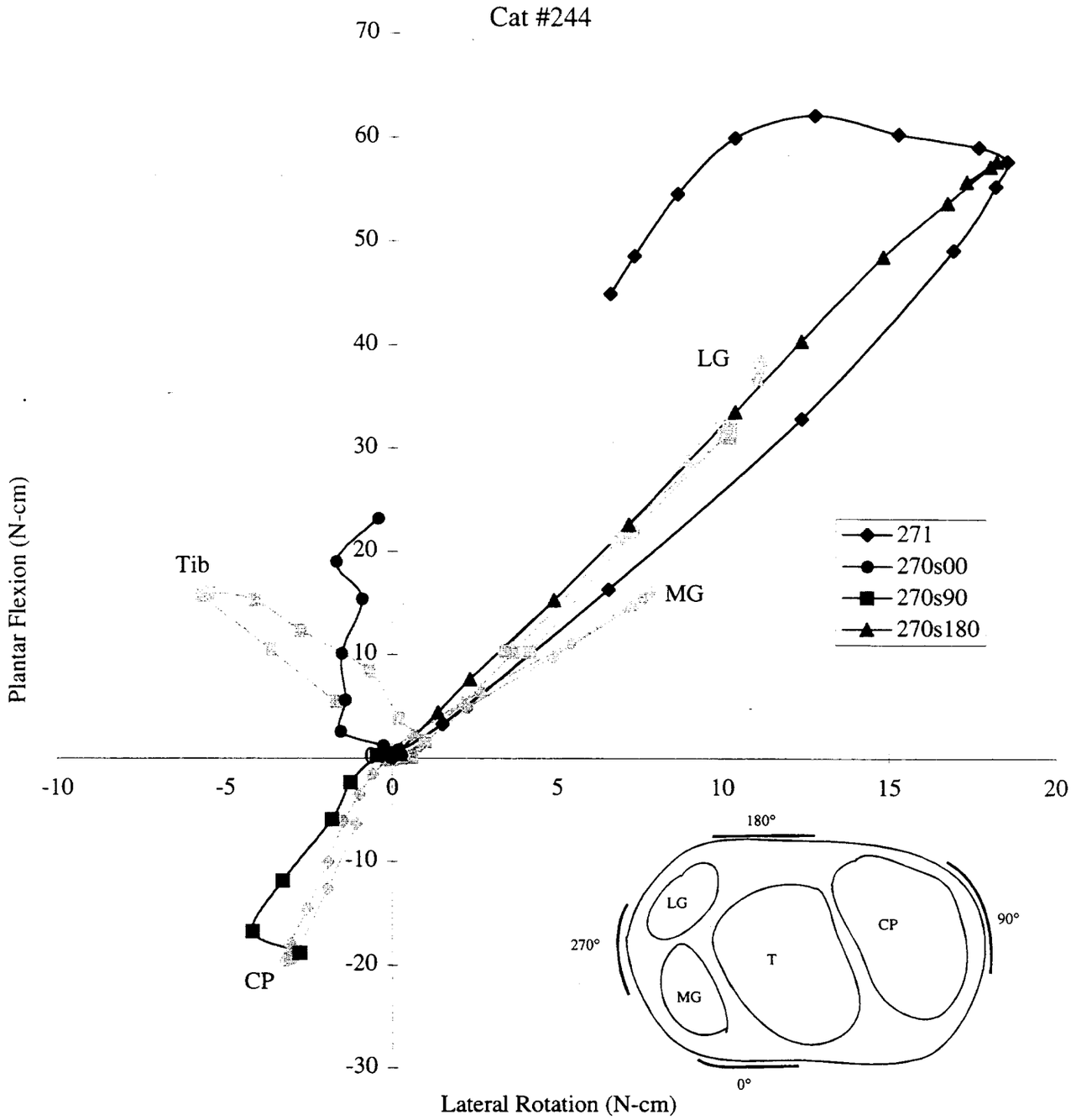


Figure 1 - Graph of torque output vectors of the ankle due to electrical stimulation from a cuff electrode around the sciatic nerve. These data show that a steering current from the 180° position shown with triangles, produces an increase in the torque output from the lateral gastrocnemius which is closer to the 180° position.

common peroneal. Finally, stimulation from the 270° position with steering from the 0° position corresponded to output found for the tibial branch combined with either the lateral or medial gastrocnemius. The reason the expected results were not achieved could be due to either experimental error or a misunderstanding of the effects of steering. The most likely experimental error would be a reversal of the stimulus polarity. This reversal of polarity would stimulate in regions not expected to be activated and not stimulate regions expected to be stimulated. Although it was not possible to completely rule out this possible source of error, there is no evidence suggesting a mistake had occurred. The order of the experiments were not consecutive or follow a configuration that would explain the output. The occurrence of this unexpected activation also occurred multiple times for different configurations.

A second experiment, shown in figure C.2, was performed with similar results. In this experiment, the contact in the 90° position was located between the medial and lateral gastrocnemius and was found to produce an output vector that bisected the medial and lateral gastrocnemius vectors, as shown in figure C.2. The addition of a positive steering current from the side (180° position) closer to the medial gastrocnemius produced selective activation of the medial gastrocnemius fascicle rather than the expected activation of the lateral gastrocnemius. This vector output is shown in figure C.2 by the curve marked with circles. The addition of positive steering current from the 0° position to the 90° position produced selective activation of the lateral gastrocnemius fascicle, as shown by the curve marked with triangles rather than the medial gastrocnemius, as expected.

In the third experiment, the 180° position was found to recruit a combination of the common peroneal and the tibial fascicles. Positive steering current from the 90° position produced the expected selective activation of the common peroneal fascicle as shown in figure C.3. The solid lines show that the 180° position contact alone produces vectors that are between the tibial and common peroneal fascicles. The dotted lines show that the addition of steering from the 90° position to the stimulation at the 180° position produces vectors that represent the common peroneal. Each different line represents a different recruitment taken at different times throughout the experiment. Although there are some variations over time, the output vector of each curve exhibit recruitment of the common peroneal before 'spilling over'.

In summary, two of the three experiments (experiments 1 and 2) found positive steering currents to produce an effect that was opposite to our expectations. Four possible explanations include, the steering current was mistakenly negative rather than positive, the

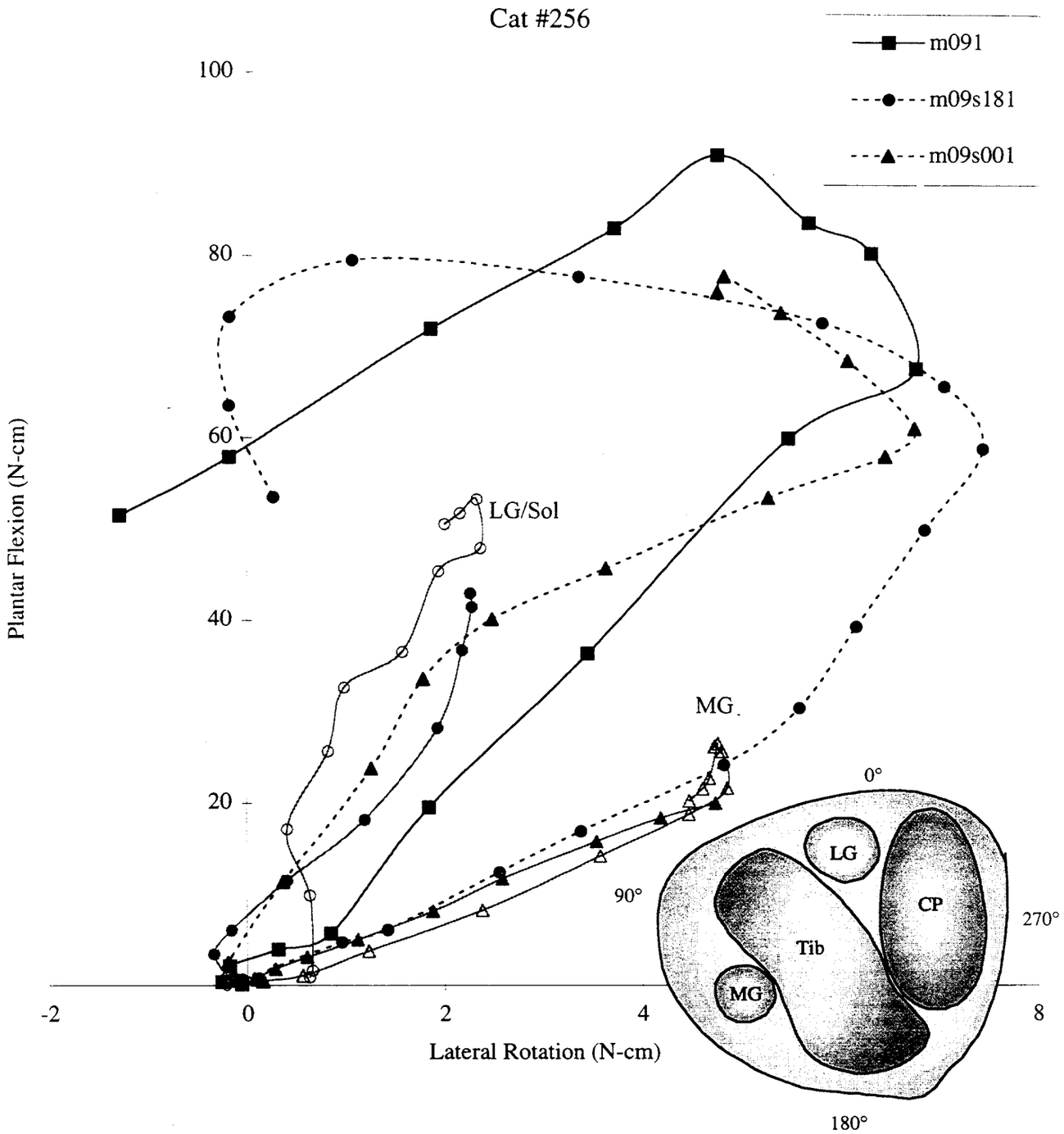


Figure 2 - Graph of the output torque vectors from the ankle due to electrical stimulation from a cuff electrode around the sciatic nerve. These data show that, although the 90° position contact alone (squares) recruits both the medial and lateral gastrocnemius. Using positive field steering current from the 180° position to the 90° position (circles) produces medial gastrocnemius output torque vectors. Using positive field steering current from the 0° position to the 90° position (triangles) produces lateral gastrocnemius output toque vectors.

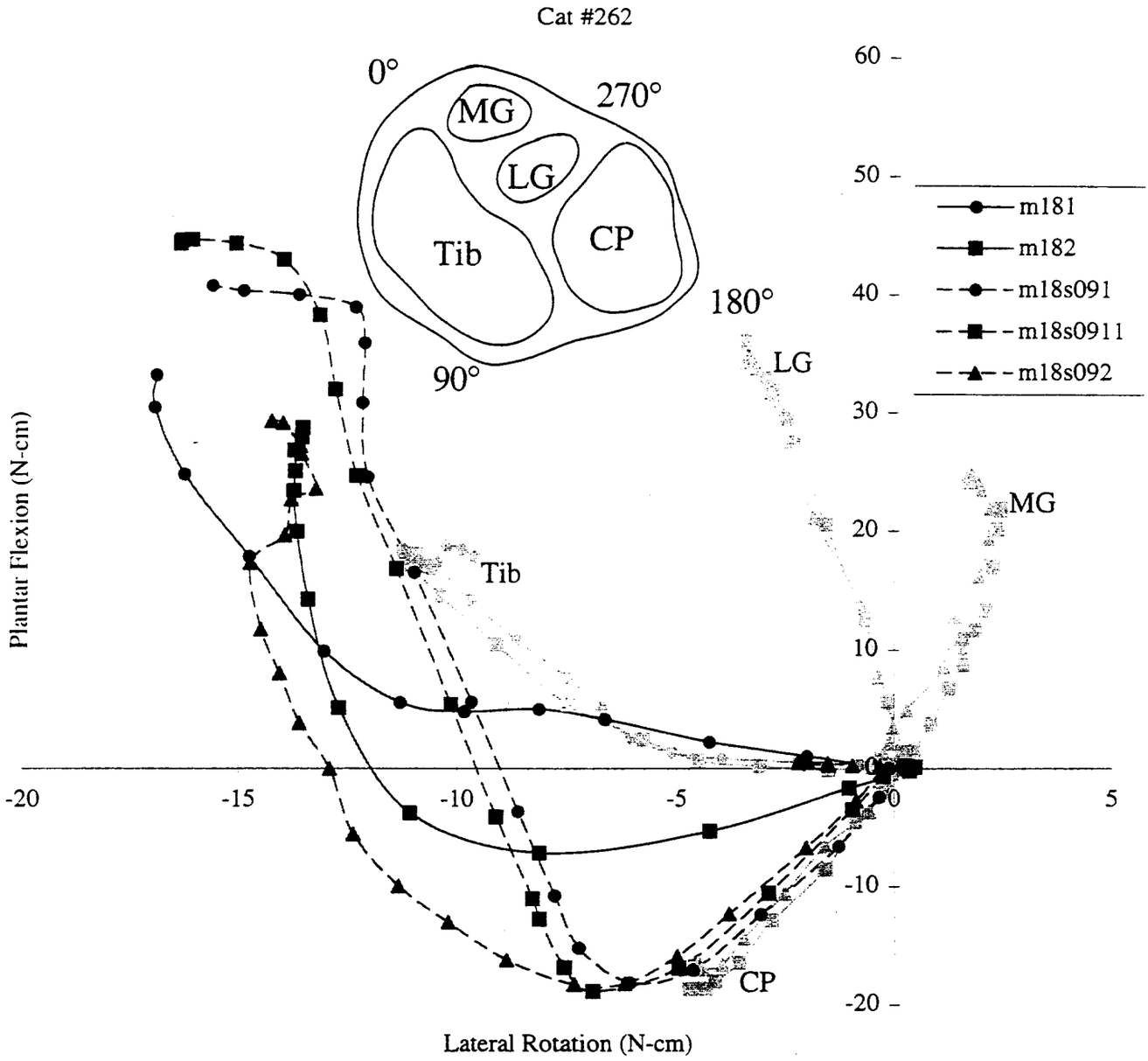


Figure 3 - Graph of the output torque vectors from the ankle due to electrical stimulation from a cuff electrode around the sciatic nerve. These data show that, although the 180° position contact alone (solid lines) does not recruit either the tibial nerve or the common peroneal nerve very well by itself, adding field steering current from the 90° position to the 180° position (dashed lines) produces common peroneal output torque vectors.

incorrect electrode contact was attached to the stimulator, the believed position of the fascicles within the nerve relative to the contacts in the nerve cuff was incorrect, or our understanding of the effect of positive steering current is not correct. We don't believe a mistake occurred for either setting the polarity of the steering currents nor the attachment of the contacts. We are beginning to explore potential maps of simulated nerve trunks to better understand current flow and the mechanisms of "field steering.

Stimulator Requirements -

An implantable stimulator that can produce "field steering", as it is now implemented, is not available. Present implementation of "field steering" produces anodic and cathodic pulses on different electrode contacts simultaneously. No present stimulator used in either upper or lower neural prostheses is capable of this output due to its technologically challenging requirements. An alternative approach, which appears to be technologically easier to implement, is to use two stimulators attached to each electrode contact, each with opposite polarization and a common return electrode.

Present experimental work produces "field steering" using two independent channels of output as shown in figure C.4. Stimulator A (in figure C.4) delivers the stimulating current between a stimulating contact and a distant reference. Stimulator B (in figure C.4) delivers the steering current between the stimulating contact and the contact from which steering is desired. Each polarity of stimulator B, therefore, must be capable of being connected to any contact inside the nerve cuff. Present stimulators (used for upper and lower neural prostheses) use independent cathodic channels with a common anode. These stimulators are not capable of imposing an anodic current on a contact.

An alternative method of producing field steering is illustrated in figure C.5. In this configuration two stimulators are required, each of which is capable of delivering current between any contact and a common return electrode. One stimulator, stimulator A in figure C.5a, delivers a cathodic pulse to the stimulating contact. The second stimulator, stimulator B in figure C.5b, has its polarity reversed and delivers an anodic pulse to the steering contact. By combining stimulators A and B, it is possible to produce a steering current. A schematic of an electrical equivalent system, showing how stimulators A and B produce these steering currents is shown in figure C.5c. When the amplitude of stimulators A and B are equal, the return currents will cancel. When the return currents cancel, all of the current will then be steering current flowing from one contact to the other contact. A schematic of this hypothesized field within the nerve is illustrated in figure

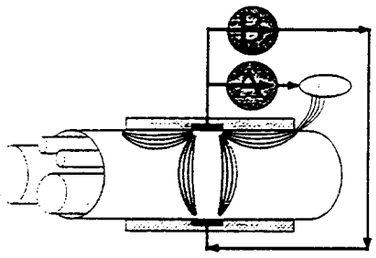

Figure C.4 - Schematic of the present configuration. Stimulator A is connected between a contact and a distant reference. Stimulator B is connected between two different contact inside the cuff.

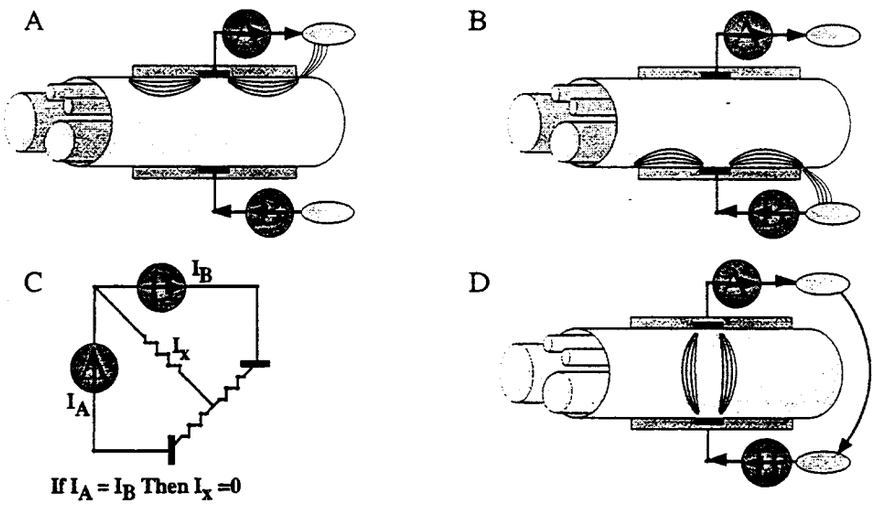


Figure C.5 - Method of using a modified set of two stimulators to produce steering current. Stimulators A and B are shown active in parts A and B respectively. Part C is a schematic of an equivalent circuit to demonstrate that if the current in A and B are equal, the Ix currents cancel resulting in only transvers current as shown in part C.

C.5d. When the amplitudes of stimulators A and B are not equal, the steering current is equal to the lesser of the two amplitudes and the remaining current is the longitudinal current. The stimulating and steering currents can therefore be set by setting the stimulator used for steering equal to the amplitude of steering desired and the stimulator used for stimulation equal to the amplitude of the steering plus the amplitude desired for stimulation. Software can be developed to handle this extra calculation, automatically adding the additional steering current to the stimulating current.

The requirement for amplitude modulation is presently addressed by a stimulator by Life Systems Inc. that is capable of 256 levels of amplitude modulation. This level of modulation is comparable to the presently used stimulator if the maximum amplitude is set to 5 mA. Ideally the maximal amplitude could be modified to provide the greatest precision for any electrode set.

It appears that this two stimulator approach will be the simplest to implement technologically. It also appears that the Life Systems Inc. stimulator could be used, with only minor modifications. Additional investigation is needed to test the efficacy of assembling the stimulators in the aforementioned configuration.